Inorg. Chem. **2009**, *48*, 1666−1677

Halogen Bonded Supramolecular Assemblies of $[Ru(bipy)(CN)_4]^{2-}$ Anions and *N*-Methyl-Halopyridinium Cations in the Solid State and in Solution

Sofia Derossi, Lee Brammer, Christopher A. Hunter, and Michael D. Ward*

Department of Chemistry, University of Sheffield, Sheffield S3 7HF, U.K.

Received November 10, 2008

The interactions between the $[Ru(bipy)(CN)_4]^{2-}$ anion and *N*-methyl-halopyridinium cations have been examined in both the solid state and in solution. In the solid state, crystal structures of $[Ru(bipy)(CN)_4]^{2-}$ salts containing iodinated cations (*N*-methyl-3-iodopyridinium and *N*-methyl-3,5-diiodopyridinium) show clear C−I···NC(Ru) halogen bonds between the externally directed cyanide lone pairs of the anion and the iodine atoms of the cation which dominates the structures. In contrast the analogous brominated cations (*N*-methyl-3-bromopyridinium and *N*-methyl-3,5-dibromopyridinium) do not exhibit C−Br···NC(Ru) interactions in the solid state, with the cyanide groups instead involved in hydrogen bonding, principally to lattice water molecules. The charge-assisted C−I···NC(Ru) interactions are therefore clearly of value as synthons in crystal engineering applications. In CH_2Cl_2 solution, spectroscopic titrations between $[Ru(4,4'\text{-}^tBu_2\text{-bipy})(CN)_4]^{2-}$ and both *N*-methyl-3-iodopyridinium and *N*-methyl-3-bromopyridinium cations show clear evidence for formation of distinct 1:1, 3:2, and then 2:1 cation/anion adducts with high association constants (>10^7 M^{-1} for the first 1:1 association constant). However the presence of identical results using the non-halogenated cation *N*-methyl-pyridinium indicates that this strong cation/anion association in CH_2Cl_2 is dominated by electrostatic effects: either C−H···NC(Ru) hydrogen bonds or C−X···NC(Ru) halogen bonds could be involved in the ion pairs but it is the charge-assistance that makes the association strong. This is confirmed by a titration between $[Ru(4,4'\text{-}^tBu_2\text{-bipy})(CN)_4]^{2-}$ and the neutral halogen-bond acceptor C_6F_5I for which the first association constant is very low (ca. 6 M^{-1}). The formation of adducts between $[Ru(4,4'\text{-}^tBu_2\text{-bipy})(CN)_4]^{2-}$ and the various *N*-methyl-pyridinium cations in solution results in a clear blue-shift of the ^{1}MLCT absorption maxima associated with the Ru(II) unit, a characteristic consequence of interaction of the cyanide lone pairs with a Lewis-acidic site on the cation. The ^{3}MLCT luminescence from the $[Ru(4,4'\text{-}^tBu_2\text{-bipy})(CN)_4]^{2-}$ center, however, does not show the usual associated increase in intensity associated with this blue shift in the ^{1}MLCT absorptions, most likely because of electron-transfer quenching by the *N*-methyl-pyridinium cations in the assemblies.

Introduction

Supramolecular assemblies, both in the solid state and in solution, rely on a range of weak, non-covalent interactions to hold the components together.[1,2] The most extensively exploited of these are labile metal−ligand coordinate bonds and hydrogen-bonding interactions,[1] both of which are relatively strong and have highly directional character, and can therefore be used to achieve some degree of geometric predictability and control in the assembly of molecular components.

An alternative interaction which has more recently become of interest as a construction tool in the field of crystal

* To whom correspondence should be addressed. E-mail: m.d.ward@sheffield.ac.uk.

(1) (a) Philp, D.; Stoddart, J. F. *Angew. Chem., Int. Ed. Engl.* **1996**, *35*, 1154. (b) Swiegers, G. F.; Malefetse, T. J. *Coord. Chem. Rev.* **2002**, *225*, 91. (c) Fujita, M.; Tominaga, M.; Hori, A.; Therrien, B. *Acc. Chem. Res.* **2005**, *38*, 369. (d) Fiedler, D.; Leung, D. H.; Bergman, R. G.; Raymond, K. N. *Acc. Chem. Res.* **2005**, *38*, 349. (e) Ward, M. D. *Chem. Soc. Rev.* **1997**, *26*, 365. (f) Desiraju, G. *Angew. Chem., Int. Ed. Engl.* **1995**, *34*, 2311. (g) Steed, J. W.; Atwood, J. L. *Supramolecular Chemistry*; Wiley: New York, 2000.

(2) (a) Desiraju, G.; Parthasarathy, R. *J. Am. Chem. Soc.* **1989**, *111*, 8725. (b) Metrangolo, P.; Neukirch, H.; Pilati, T.; Resnati, G. *Acc. Chem. Res.* **2005**, *38*, 386. (c) Metrangolo, P.; Meyer, F.; Pilati, T.; Resnati, G.; Terraneo, G. *Angew. Chem., Int. Ed.* **2008**, *47*, 6114. (d) Rissanen, K. *CrystEngComm* **2008**, *10*, 1107. (e) Brammer, L.; Mínguez Espallargas, G.; Libri, S. *CrystEngComm* [Online early access]. DOI: 10.1039/b812927d. Published Online: **2008**, *10*, in press.

10.1021/ic8021529 CCC: $40.75
Published on Web 01/09/2009

engineering is the halogen bond.[2−5] It has been shown that carbon-halogen groups (C−X; X = Cl, Br, I) and neutral dihalogens (X_2) form halogen bonding interactions X···B with a range of organic bases (B),[3,4] with 1:1 association constants in non-polar solvents being typically in the range 10^0-10^3 M^{-1}.[3f] Iodo- and bromoperfluoroaromatic and -aliphatic molecules in particular have been exploited as halogen bond donors in supramolecular assembly for a range of applications.[4] The potential of halogen bonds as a tool for crystal engineering in inorganic chemistry[2e] has been developed by some of us who have shown that suitably activated C−X groups can form robust, directional supramolecular synthons (C−X···X′−M) when combined with halide ligands and are effective in the synthesis of organic−inorganic networks involving either charged or neutral coordination compounds.[5] The geometries associated with such assemblies are consistent with electrophile-nucleophile interactions in which the inorganic halogen (M−X) plays the nucleophilic role and the organic halogen is the electrophile.[5] Ab initio and density-functional theory (DFT) calculations have confirmed the importance of electrostatic forces in providing both an attractive and a directional C−X···X′−M interaction, and solution phase binding studies have shown that such interactions can be of comparable strength to strong hydrogen bonds.[5e]

Given the simple electrostatic correspondence between metal-halide and metal-pseudohalide groups, the related C−X···NC−M interaction, between an externally directed lone pair of electrons in a cyanometallate anion and an electrophilic halogen atom in an organic molecule, can likewise provide a basis for constructing supramolecular assemblies. Examples of the use of C−X···NC−M interactions to control assembly of crystalline materials are very limited, with the few structurally characterized examples being materials in which cyanometallate anions and halogenated thiafulvalene anions are combined to afford materials with desirable conductivity or magnetic properties.[6] Our recent experience in developing halogen bonds with metal halides providing the nucleophilic partner,[5] when considered alongside known interactions of metal cyanides, strongly suggests that tunable C−X···NC−M interactions could be developed for applications in crystal synthesis and possibly also in facilitating formation of supramolecular assemblies in solution.

The impetus for this work comes from recent studies on luminescent cyanometallate anions such as [Ru(bipy)-(CN)$_4$]$^{2-}$ and [Os(bipy)(CN)$_4$]$^{2-}$, and their simple derivatives and polynuclear analogues, which have proven to be of considerable value in supramolecular photochemistry.[7−9] Their externally directed cyanide lone pairs provide a means for incorporating these chromophores into coordination networks (via coordination of the cyanides to different metal cations) and hydrogen-bonded assemblies; and this involvement of the cyanide lone pairs in interactions with external electron-accepting groups results in substantial changes to the photophysical properties of the cyanometallate anions which are accordingly highly environment-sensitive.[7−10] The cyanide groups therefore simultaneously (i) provide a means for cyanometallate luminophores to combine with other components, and (ii) report on the interaction by causing a modification of the spectroscopic properties of the chromophore.

Accordingly in this paper we report a structural and solution phase study on the combination of [Ru(bipy)-(CN)$_4$]$^{2-}$ anions with cationic organohalogen compounds, and demonstrate how cyanide-halogen interactions are a useful addition to the supramolecular chemist's armory for preparation of multicomponent assemblies. The solid-state structures

(3) (a) Castellote, I.; Morón, M.; Burgos, C.; Alvarez-Builla, J.; Martin, A.; Gómez-Sal, P.; Vaquero, J. J. *Chem. Commun.* **2007**, 1281. (b) Bouchmella, K.; Boury, B.; Dutremez, S. G.; van der Lee, A. *Chem.—Eur. J.* **2007**, *13*, 6130. (c) Lu, Y.-X.; Zou, J.-W.; Wang, Y.-H.; Yu, Q.-S. *Chem. Phys.* **2007**, *334*, 1. (d) Lucassen, A. C. B.; Karton, A.; Leitus, G.; Shimon, L. J. W.; Martin, J. M. L.; van der Boom, M. E. *Cryst. Growth Des.* **2007**, *7*, 386. (e) Laurence, C.; Queignec-Cabanetos, M.; Dziembowska, T.; Queignec, R.; Wojtkowiak, B. *J. Am. Chem. Soc.* **1981**, *103*, 2567. (f) Laurence, C.; Queignec-Cabanetos, M.; Wojtkowiak, B. *J. Chem. Soc., Perkin Trans II* **1982**, 1605. (g) Lu, Y.-X.; Zou, J.-W.; Wang, Y.-H.; Jiang, Y.-J.; Yu, Q.-S. *J. Phys. Chem. A* **2007**, *111*, 10781. (h) Lu, Y.-X.; Zou, J.-W.; Wang, Y.-H.; Yu, Q.-S. *J. Mol. Struct.: THEOCHEM* **2006**, *767*, 139. Rimmer, E. L.; Bailey, R. D.; Hanks, T. W.; Pennington, W. T. *Chem.—Eur. J.* **2000**, *6*, 4071. (i) Padgett, C. W.; Walsh, R. D.; Drake, G. W.; Hanks, T. W.; Pennington, W. T. *Cryst. Growth Des.* **2005**, *5*, 745. (j) Pennington, W. T.; Hanks, T. W.; Arman, H. D. *Struct. Bonding (Berlin)* **2008**, *126*, 65. (k) Saha, B. K.; Nangia, A.; Jaskólski, M. *CrystEngComm* **2005**, *7*, 355.

(4) (a) Corradi, E.; Meille, S. V.; Messina, M. T.; Metrangolo, P.; Resnati, G. *Angew. Chem., Int. Ed.* **2000**, *39*, 1782. (b) Corradi, E.; Meille, S. V.; Messina, M. T.; Metrangolo, P.; Resnati, G. *Angew. Chem., Int. Ed.* **2000**, *39*, 1782. (c) Metrangolo, P.; Pilati, T.; Resnati, G.; Stevenazzi, A. *Chem. Commun.* **2004**, 1492. (d) Caronna, T.; Liantonio, R.; Logothetis, T. A.; Metrangolo, P.; Pilati, T.; Resnati, G. *J. Am. Chem. Soc.* **2004**, *126*, 4500. (e) Mele, A.; Metrangolo, P.; Neukirch, H.; Pilati, T.; Resnati, G. *J. Am. Chem. Soc.* **2005**, *127*, 14972.

(5) (a) Mínguez Espallargas, G.; Brammer, L.; Sherwood, P. *Angew. Chem., Int. Ed.* **2006**, *45*, 435. (b) Zordan, F.; Brammer, L. *J. Am. Chem. Soc.* **2005**, *127*, 5979. (c) Zordan, F.; Brammer, L. *Cryst. Growth Des.* **2006**, *6*, 1374. (d) Zordan, F.; Minguez Espallargas, G.; Brammer, L. *CrystEngComm.* **2006**, *8*, 425. (e) Libri, S.; Jasim, N. A.; Perutz, R. N.; Brammer, L. *J. Am. Chem. Soc.* **2008**, *130*, 7842. (f) Mínguez Espallargas, G.; Brammer, L.; Allan, D. R.; Pulham, C. R.; Robertson, N.; Warren, J. E. *J. Am. Chem. Soc.* **2008**, *130*, 9058.

(6) (a) Fourmigué, M.; Batail, P. *Chem. Rev.* **2004**, *104*, 5379. (b) Ranganathan, A.; El-Ghayoury, A.; Mézière, C.; Harté, E.; Clérac, R.; Batail, P. *Chem. Commun.* **2006**, 2878. (c) Imakubo, T.; Sawa, H.; Kato, R. *J. Chem. Soc., Chem. Commun.* **1995**, 1667. (d) Imakubo, T.; Tajima, N.; Tamura, M.; Kato, R.; Nishio, Y.; Kajita, K. *J. Mater. Chem.* **2002**, *12*, 159. (e) Ouahab, L.; Setifi, F.; Golhen, S.; Imakubo, T.; Lescouezec, R.; Lloret, F.; Julve, M.; Swietlik, R. *C. R. Chim.* **2005**, *8*, 1286.

(7) Ward, M. D. *Coord. Chem. Rev.* **2006**, *250*, 3128.

(8) (a) Davies, G. M.; Pope, S. J. A.; Adams, H.; Faulkner, S.; Ward, M. D. *Inorg. Chem.* **2005**, *44*, 4656. (b) Herrera, J.-M.; Pope, S. J. A.; Adams, H.; Faulkner, S.; Ward, M. D. *Inorg. Chem.* **2006**, *45*, 3895. (c) Adams, H.; Alsindi, W. Z.; Davies, G. M.; Duriska, M. B.; Easun, T. L.; Fenton, H. E.; Herrera, J.-M.; George, M. W.; Ronayne, K. L.; Sun, X.-Z.; Towrie, M.; Ward, M. D. *Dalton Trans.* **2006**, 39. (d) Herrera, J.-M.; Pope, S. J. A.; Meijer, A. J. H. M.; Easun, T. L.; Adams, H.; Alsindi, W. Z.; Sun, X.-Z.; George, M. W.; Faulkner, S.; Ward, M. D. *J. Am. Chem. Soc.* **2007**, *129*, 11491. (e) Lazarides, T.; Easun, T. L.; Veyne-Marti, C.; Alsindi, W. Z.; George, M. W.; Deppermann, N.; Hunter, C. A.; Adams, H.; Ward, M. D. *J. Am. Chem. Soc.* **2007**, *129*, 4014. (f) Baca, S. G.; Adams, H.; Grange, C. S.; Smith, A. P.; Sazanovich, I.; Ward, M. D. *Inorg. Chem.* **2007**, *46*, 9779. (g) Baca, S. G.; Pope, S. J. A.; Adams, H.; Ward, M. D. *Inorg. Chem.* **2008**, *47*, 3736.

(9) (a) Pina, F.; Parola, A. J. *Coord. Chem. Rev.* **1999**, *185−186*, 149. (b) Bergamini, G.; Saudan, C.; Ceroni, P.; Maestri, M.; Balzani, V.; Gorka, M.; Lee, S.-K.; van Heyst, J.; Vögtle, F. *J. Am. Chem. Soc.* **2004**, *126*, 16466. (c) Indelli, M. T.; Ghirotti, M.; Prodi, A.; Chiorboli, C.; Scandola, F.; McClenaghan, N. D.; Puntoriero, F.; Campagna, S. *Inorg. Chem.* **2003**, *42*, 5489.

Table 1. Crystal Parameters, Data Collection, and Refinement Details for the Five Crystal Structures in this Paper

complex	[*N*-Me-C_5H_5N]$_2$ [Ru(bipy)(CN)$_4$]·H_2O (**1**·H_2O)	[*N*-Me-3-I-C_5H_4N]$_2$ [Ru(bipy)(CN)$_4$]· 0.5(MeCN) [**2**·0.5(MeCN)]	[*N*-Me-3,5-I_2-C_5H_3N]$_2$ [Ru(bipy)(CN)$_4$] (**3**)	[*N*-Me-3-Br-C_5H_4N]$_2$ [Ru(bipy)(CN)$_4$]· $2H_2O$ (**4**·$2H_2O$)	[*N*-Me-3,5-Br_2-C_5H_3N]$_2$ [Ru(bipy)(CN)$_4$]·$5H_2O$[b] (**5**·$5H_2O$)
formula	$C_{26}H_{26}N_8ORu$	$C_{27}H_{23.5}I_2N_{8.5}Ru$	$C_{26}H_{20}I_4N_8Ru$	$C_{27}H_{26}Br_2N_8O_2Ru$	$C_{26}H_{30}Br_4N_8O_5Ru$
molecular weight	567.62	821.91	1053.17	743.44	955.29
T, K	100(2)	100(2)	100(2)	100(2)	130(2)
crystal system	monoclinic	monoclinic	triclinic	monoclinic	monoclinic
space group	$P2_1/n$	$P2_1/n$	$P\bar{1}$	$P2_1/n$	$P2_1$
a, Å	8.8686(6)	17.885(4)	9.3350(8)	8.946(1)	11.8193(6)
b, Å	32.668(2)	9.529(2)	13.1418(2)	31.484(4)	11.2662(6)
c, Å	9.2236(7)	33.780(7)	13.7330(13)	10.128(2)	12.6933(6)
α, deg	90	90	113.435(5)	90	90
β, deg	114.480(4)	91.59(3)	90.038(5)	102.987(6)	93.502(3)
γ, deg	90	90	100.223(5)	90	90
V, Å^3	2432.0(3)	5755(2)	1516.5(2)	2779.5(7)	1687.1(2)
Z	4	8	2	4	2
ρ, g cm^{-3}	1.550	1.897	2.306	1.777	1.881
μ, mm^{-1}	0.682	2.724	4.620	3.479	5.249
data, restraints, parameters	9689, 2, 320	12583, 2, 712	6411, 0, 352	8488, 0, 342	7511, 1, 399
final *R*1, *wR2*[a]	0.0446, 0.1052	0.0422, 0.1031	0.0549, 0.1589	0.0355, 0.0837	0.0328, 0.0723

[a] $R1 = \sum||F_o| - |F_c||/\sum|F_o|$ for "observed data"; $wR2 = [\sum w(F_o^2 - F_c^2)^2/\sum w(F_o^2)^2]^{1/2}$ for all unique data. [b] This structure is an a noncentrosymmetric space group; Flack parameter = 0.022(6).

indicate that charge-assisted C−X···NC−M halogen-bonding interactions play a major role in controlling the solid-state structures for X = I, but not for X = Br. Solution studies show that strong binding between [Ru(^{t}Bu$_2$bipy)-(CN)$_4$]$^{2-}$ anions and the organohalogen cations occur with comparable strength irrespective of the nature of the halogen, implying that in solution the electrostatic ion-pairing effect plays a much more significant role in the association process than the specific nature of the halogen.

Results and Discussion

Crystal Structures. Salts of [Ru(bipy)(CN)$_4$]$^{2-}$ were prepared by salt metathesis using a series of organohalogen cations. *N*-methyl-3-bromopyridinium, *N*-methyl-3-iodopyridinium, *N*-methyl-3,5-dibromopyridinium and *N*-methyl-3,5-diiodopyridinium were used, all as their hexafluorophosphate or tetrafluoroborate salts; previous calculations have established the electrophilic character of the halogen atoms in 3-substituted halopyridinium ions.[5a,b] As a control we also employed *N*-methylpyridinium hexafluorophosphate, in which there are no halogen substituents on the cation. Slow mixing of solutions of these salts with a solution of (PPN)$_2$-[Ru(bipy)(CN)$_4$][11] in CH_2Cl_2 afforded in every case a precipitate which contained mostly amorphous material but mixed with a small number of dark red X-ray quality single crystals. In every case described below, the bond distances and angles in the methylpyridinium cations and [Ru(bipy)(CN)$_4$]$^{2-}$ anions are unremarkable; the features of interest are the non-covalent interactions, for which metric parameters are discussed in the main text. Crystallographic data are summarized in Table 1.

To start with, we used the non-halogenated *N*-methylpyridinium cation to prepare crystals of [*N*-methylpyridinium]$_2$[Ru(bipy)(CN)$_4$]·H_2O (**1**·H_2O, Figures 1 and 2). In this case the sole water of crystallization *per* formula unit forms hydrogen bonds to cyanide atoms N(1) and N(4) from different complex anions, linking them into a hydrogen-bonded chain [N(1)···O(1), 2.962(3) Å; N(4)···O(1), 2.893(3) Å] (Figure 2). The other two cyanide N atoms are involved solely in C−H···N hydrogen-bonding interactions with

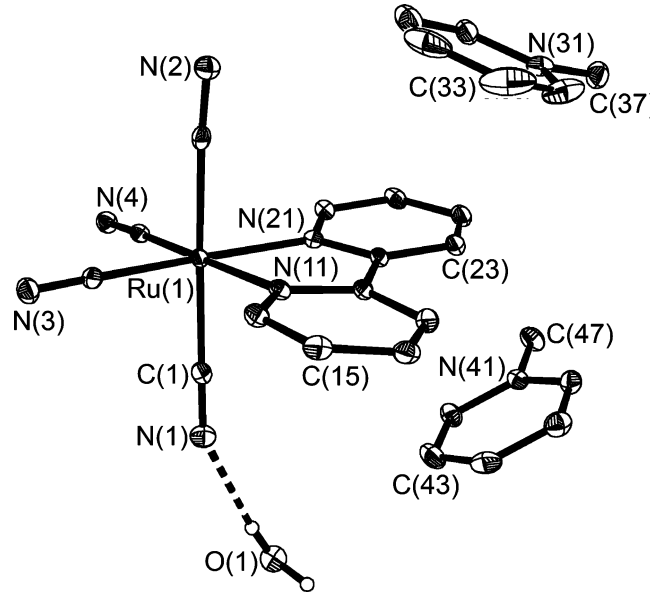

Figure 1. Asymmetric unit of [*N*-methylpyridinium]$_2$[Ru(bipy)(CN)$_4$]·H_2O (**1**·H_2O) showing the atomic numbering scheme. Hydrogen atoms other than those of the water molecule are not shown. Thermal ellipsoids are at the 40% probability level.

N-methylpyridinium cations. The methyl groups in particular offer multiple sites for such interactions. There are no noticeable aromatic stacking interactions between cations and anions.

In [*N*-methyl-3-iodopyridinium]$_2$[Ru(bipy)(CN)$_4$]·0.5(MeCN)[**2**·0.5(MeCN), Figures 3 and 4], the asymmetric unit contains two inequivalent [Ru(bipy)(CN)$_4$]$^{2-}$ anions and four cations. Each [Ru(bipy)(CN)$_4$]$^{2-}$ anion is associated with two *N*-methyl-3-iodopyridinium cations by C−I···NC(Ru) halogen bonds (Figure 4), with N···I separations all lying in the range 2.81−2.96 Å, corresponding to normalized distances of $0.80 < R_{NI} < 0.84$,[12] that is, much less than the sum of the van der Waals radii for these two atoms (3.53 Å; $R_{NI} = 1.00$). Consistent with strong halogen bonds all

(10) Timpson, C. J.; Bignozzi, C. A.; Sullivan, B. P.; Kober, E. M.; Meyer, T. J. *J. Phys. Chem.* **1996**, *100*, 2915.
(11) Evju, J. K.; Mann, K. R. *Chem. Mater.* **1999**, *11*, 1425.

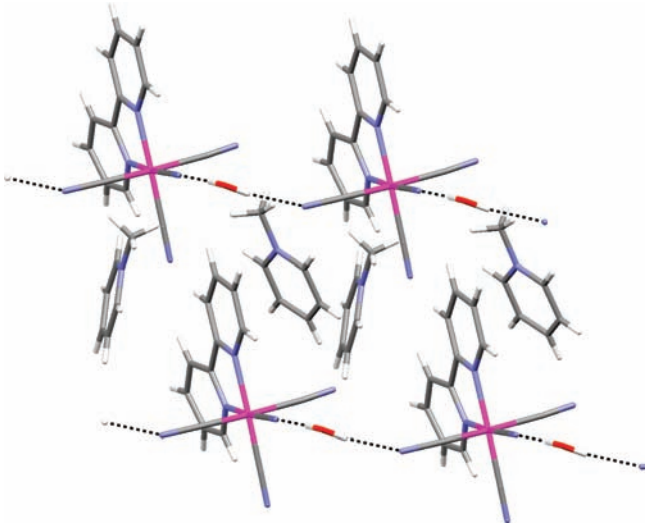

Figure 2. Crystal structure of [*N*-methylpyridinium]$_2$[Ru(bipy)(CN)$_4$]·H$_2$O (**1**·H$_2$O) showing O−H···NC(Ru) hydrogen-bonded network.

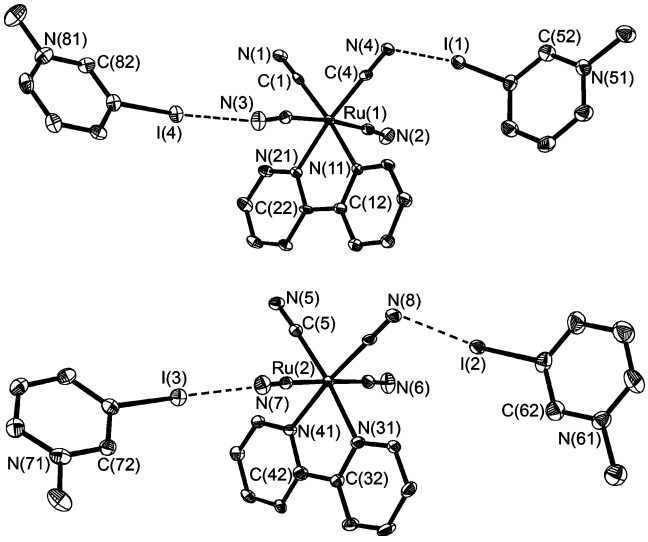

Figure 3. Atomic labeling for anions and cations in the crystal structure of [*N*-methyl-3-iodopyridinium]$_2$[Ru(bipy)(CN)$_4$]·0.5(MeCN) [**2**·0.5(MeCN)]. C−I···NC(Ru) halogen bonds are indicated with dashed lines. Disordered acetonitrile molecule not shown. Thermal ellipsoids are at the 40% probability level.

C−I···N angles are close to linearity [171.4(2)−179.2(2)°]. In each case a *cis*-related pair of cyanide ligands on the complex anion is involved, one axial and one equatorial, with the C−I···NC(Ru) interaction involving the axial cyanide being near-linear at the cyanide [C−N···I angles, 163.4(5)° at N(3) and 161.5(4)° at N(7)] and the interaction involving the equatorial cyanide being more bent [C−N···I angles, 126.0(4)° at N(4) and 125.0(4)° at N(8)]. It is noticeable that these two more bent C−N···I geometries are associated with the two longest N···I separations [2.964(5) Å at N(4) and 2.905(5) Å at N(8)] whereas the two more nearly linear

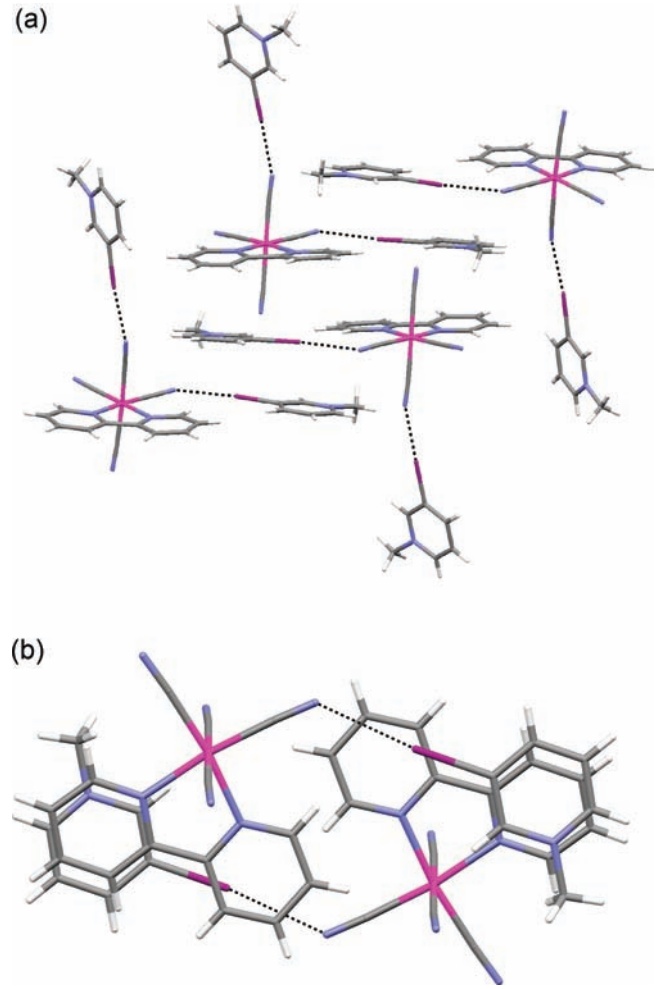

Figure 4. Crystal structure of [*N*-methyl-3-iodopyridinium]$_2$[Ru(bipy)(CN)$_4$]·0.5(MeCN) [**2**·0.5(MeCN)] showing the combination of (a) C−I···NC(Ru) halogen bonds and (b) aromatic π-stacking interactions.

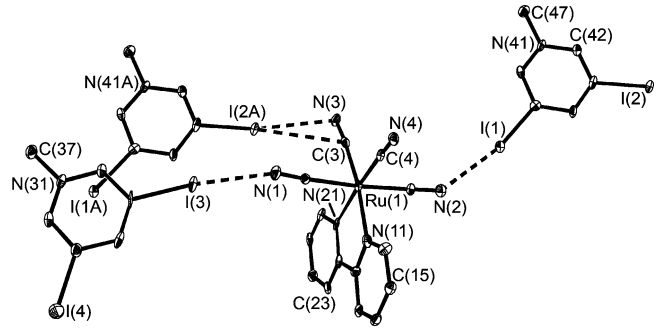

Figure 5. Atomic labeling for anions and cations in crystal structure of [*N*-methyl-3,5-diiodopyridinium]$_2$[Ru(bipy)(CN)$_4$] (**3**). The C−I···NC(Ru) and C−I···π(NC) halogen bonds are indicated with dashed lines. Thermal ellipsoids are at the 40% probability level.

C−N···I geometries involve shorter N···I separations [2.809(5) Å at N(3) and 2.820(6) Å at N(7)].

In addition there are aromatic π-stacking interactions between the *N*-methyl-3-iodopyridinium groups and the bipy ligands of the [Ru(bipy)(CN)$_4$]$^{2-}$ anions, as is evident in Figure 4b. In each case a cation is associated via a C−I···NC interaction with one complex anion, while being involved in a π-stacking interaction with the coordinated bipyridyl ligand of a separate complex anion. Cation−anion interac-

(12) (a) The normalized distance R_{NI} involves normalization relative to the sum of van der Waals radii of the two interacting atoms, following the definition used by Lommerse et al.,[12b] $R_{NI} = d(N\cdots I)/(r_N + r_I)$, where r_N and r_I are the van der Waals radii[12c] of nitrogen (1.55 Å) and iodine (1.98 Å), respectively. (b) Lommerse, J. P. M.; Stone, A. J.; Taylor, R.; Allen, F. H. *J. Am. Chem. Soc.* **1996**, *118*, 3108. (c) Bondi, A. *J. Phys. Chem.* **1964**, *68*, 441.

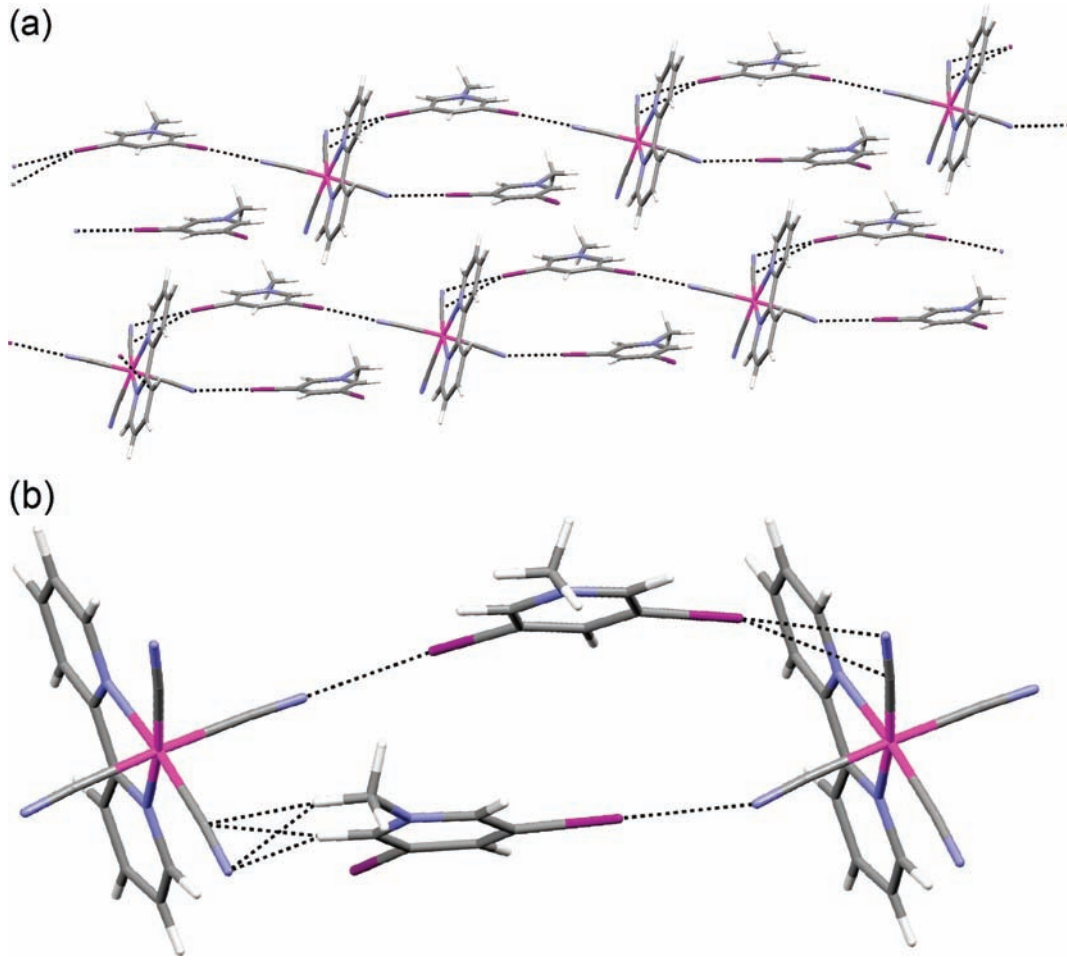

Figure 6. (a) Crystal structure of [*N*-methyl-3,5-diiodopyridinium]$_2$[Ru(bipy)(CN)$_4$] (**3**) showing the network propagated by C−I···NC(Ru) and C−I···π(NC) halogen bonds. (b) Enlarged view of part of the network showing the halogen bonds and the C−H···π(NC) hydrogen bonds.

tions are also propagated through a network of C−H···N hydrogen bonds.

In [*N*-methyl-3,5-diiodopyridinium]$_2$[Ru(bipy)(CN)$_4$] (**3**; Figures 5 and 6) the presence of two iodine atoms on the cation means that (i) there are four iodine atoms per [Ru(bipy)(CN)$_4$]$^{2-}$ anion, that is, one per cyanide group, such that potentially all cyanide groups could be involved in C−I···NC(Ru) halogen bonds; and (ii) we have the possibility of infinite networks in which cations and anions are linked by these interactions, with the *N*-methyl-3,5-diiodopyridinium cations acting as bridging units between two complex anions, which themselves could be four-connected. The structure (Figure 6) reveals that there are three C−I···NC(Ru) interactions per formula unit, with one cyanide group [N(4)] and one iodine atom [I(4)] not participating in such an interaction. All three halogen bonds show close to linear C−I···N angles and short I···N separations [for I(3)···N(1), 174.0(3)° and 2.793(7) Å (R_{NI} 0.79); for I(1)···N(2), 166.4(3)° and 2.907(7) Å (R_{NI} 0.82); for I(2)···N(3), 169.0(3)° and 2.974(7) Å (R_{NI} 0.84)]. The former two interactions show some deviation from linearity of the interaction at nitrogen, with C−N···I angles of 152.7(6) and 143.9(6)°, whereas the latter has an almost orthogonal approach of the C−I group to the cyanide ligand [C−N···I 104.9(6)° at N(3)] indicative of interaction with the C≡N triple bond rather than the nitrogen lone pair. This is supported by the correspondingly short I(2)···C(3) separation of 3.461(8) Å (R_{CI} 0.94). As in complex **1**, the more highly bent C−N···I geometries correlate with increasing N···I separation.

The involvement of both iodine atoms [I(1) and I(2)] from the same *N*-methyl-3,5-diiodopyridinium cation in interactions to cyanide groups of different complex anions results in formation of a one-dimensional chain of alternating cations and anions (Figure 6) via C−I···NC(Ru) and C−I···π(CN) halogen bonds. In contrast, for the alternate cation, only one iodine atom [I(3)] is involved in halogen bonding. However, a very similar propagation of the anion-cation chain arises in which C−H···π(CN) hydrogen bonds, involving both the methyl protons and one aromatic ring proton from the cation,[13] replace the C−I···π(CN) halogen bond (Figure 6b).

(13) (a) The methyl hydrogen atom forms shorter C−H···π(CN) hydrogen bonds (H···N 2.255 Å; H···C 2.398 Å) than the ring hydrogen atom (H···N 2.713 Å; H···C 2.708 Å). (b) In addition to the halogen bonds and hydrogen bonds observed here, simple Lewis acids such as alkali metal cations have been shown to interact side-on with coordinated cyanide ligands, i.e., with the C≡N bond rather than the nitrogen lone pair, see refs 8a and 8e.

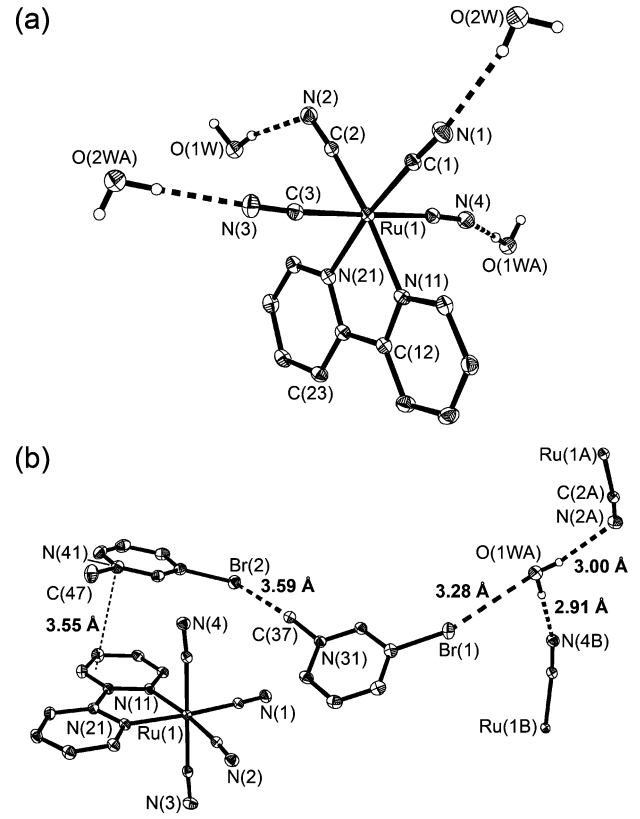

Figure 7. Atomic labeling scheme for the structure of [*N*-methyl-3-bromopyridinium]$_2$ [Ru(bipy)(CN)$_4$]·2H$_2$O (**4**·2H$_2$O), with the principal non-covalent interactions shown by dashed lines; distances given are between heavy (non-H) atoms. Thermal ellipsoids are at the 40% probability level.

The remaining iodine atom I(4) forms no significant short contacts.[14]

Replacement of iodine by bromine completely changes the structures which are now hydrated and dominated by HOH···NC(Ru) hydrogen bonds. In the structure of [*N*-methyl-3-bromopyridinium]$_2$[Ru(bipy)(CN)$_4$]·2H$_2$O (**4**·2H$_2$O; Figures 7 and 8) it is immediately apparent that there are no short CN···Br contacts. Instead, all four cyanide groups of the [Ru(bipy)(CN)$_4$]$^{2-}$ anion are involved in hydrogen-bonding interactions to water molecules (Figure 7), with H···O separations in the range 1.90−2.04 Å. Each water molecule uses its two H atoms to interact with cyanide groups from different anions; hence, two water molecules provide the necessary four H-bond donor sites. The result is a 2D hydrogen-bonded network involving every cyanide group and every water proton.

One of the two independent *N*-methyl-3-bromopyridinium cations forms no halogen bonds, but lies nearly parallel to (8° between mean planes), and is involved in a stacking interaction with, one of the coordinated pyridyl rings of a [Ru(bipy)(CN)$_4$]$^{2-}$ anion. The aromatic rings involved are offset from one another such that the cationic N atom of the pyridinium ring lies approximately above the center of the π-cloud of a coordinated pyridine ring in the complex anion. The other cation interacts via a C−Br···O halogen bond with a lone pair of one of the two water molecules [Br(1)···O(1W), 3.279(2) Å (R_{BrO} 0.97); C−Br···O angle, 163.8(1)° at Br(1)]. The coordination sphere of both water molecules is completed by C−H···O hydrogen bonds (Figure 8). The formation of halogen bonds in which water provides the halogen bond acceptor are uncommon. Only 22 crystal structures were found in the Cambridge Structural Database (CSD)[15] with apparent C−X···O halogen bonds involving water molecules (X = I, 12 structures; X = Br, 10 structures). The uncommon nature of such an interaction is highlighted by an earlier study in which water molecules insert into N−H···Cl(Pt) hydrogen bonds but do not interrupt C−X···Cl(Pt) halogen bonds in the crystal structures of (3-halopyridinium)$_2$[PtCl$_6$]·2H$_2$O.[16]

In the crystal structure of [*N*-methyl-3,5-dibromopyridinium]$_2$[Ru(bipy)(CN)$_4$]·5H$_2$O (**5**·5H$_2$O; Figures 9 and 10) the anions participate, via the cyanide ligands, in separate hydrogen-bonded and halogen-bonded networks, involving the water molecules and the cations, respectively (Figure 10). The five independent water molecules are linked in a hydrogen-bonded chain [O···O separations range from 2.677(5) to 2.977(7) Å], and three of the water molecules from one chain collectively participate in further hydrogen bonds with the four independent cyanide ligands, one from each of four independent complex anions [O···N separations range from 2.783(7) to 2.844(6) Å]. Thus each anion participates in hydrogen bonds with four separate water chains. The cations lie in approximately coplanar arrangements in between, and parallel to, the mean planes of the coordinated bipyridine ligands of the anions. The interplanar angles between the two independent cations and the bipy ligand are 7.7° and 10.5°. Conventional aromatic π-stacking does not appear to be involved, however, because of the offset of the π-systems involved. The cations in each layer engage in C−Br···Br halogen bonds involving all bromine atoms to form zigzag chains. There are two crystallographically independent but geometrically similar chains, one involving each of the independent cations. On each cation one bromine atom serves as a halogen bond donor [C−Br···Br 172.8(2), 157.0(2)° for the chain involving Br(1) and Br(2)] and the other as a halogen bond acceptor [Br···Br−C 101.6(1), 100.9(1)° for the chain involving Br(3) and Br(4)]. In addition each bromine atom that serves as an *acceptor* of a C−Br···Br halogen bond also serves as a halogen bond *donor* to a cyanide ligand of an anion. Given that the cations are approximately coplanar with the bipy ligands of the anions it is not surprising that these cation−anion halogen bonds comprise an interaction orthogonal to the cyanide ligand, which might best be described as C−Br···π(CN) halogen bonds [Br(3)···N(1), 3.188(5), R_{BrN} 0.94; Br(1)···N(2), 3.285(6), R_{BrN} 0.97; C−Br···N angles 165.5(2)° at Br(1), 166.7(2)° at Br(3); Br···N−C angles 101.6(3)° at N(1), 99.7(4)° at N(2)].

The comparison between the two sets of structures, with iodinated (complexes **2**, **3**) versus all other cations (**1**, **4**, **5**), is interesting. In no case were precautions taken to

(14) The closest interaction is with the C−H group of a neighboring anion (H···I 3.13 Å, R_{HI} 0.99).

(15) (a) Allen, F. H. *Acta Crystallogr.* **2002**, *B58*, 380. (b) Geometric restrictions on the database search were X···O < 3.5 Å and C−X···O ≥ 140°.

(16) Zordan, F.; Brammer, L. *Acta Crystallogr.* **2004**, *B60*, 512.

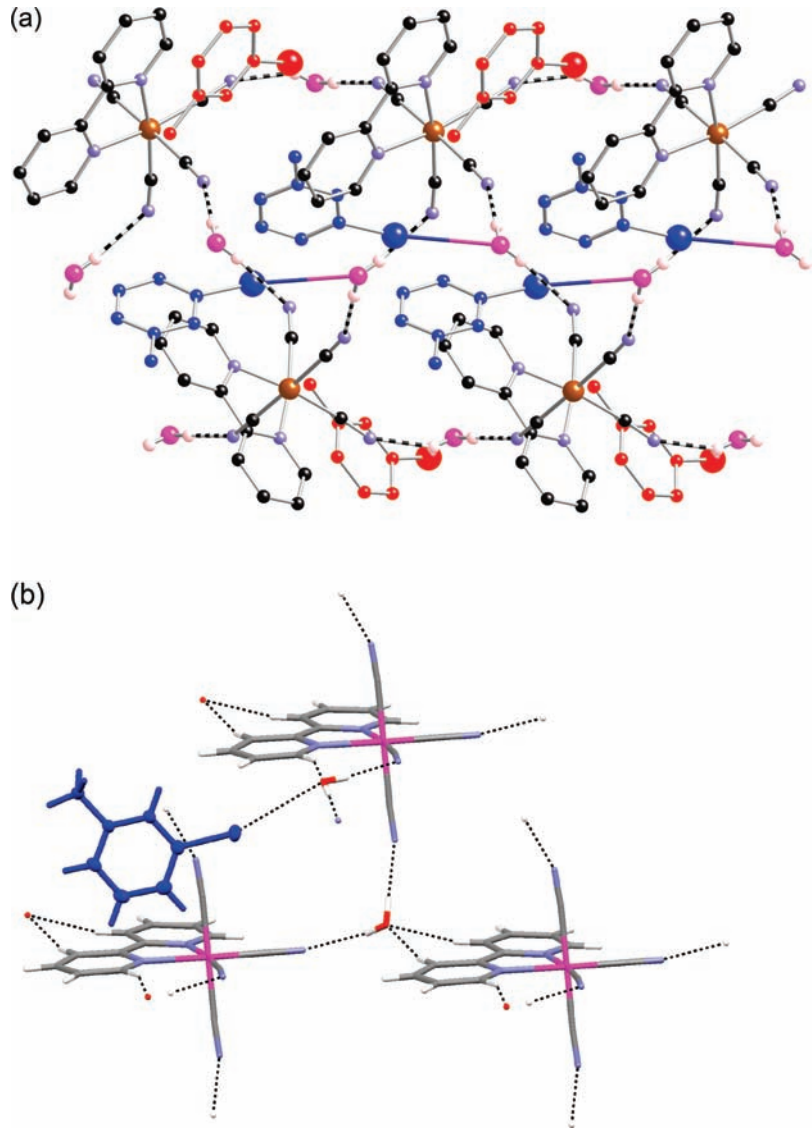

Figure 8. (a) Crystal structure of [*N*-methyl-3-bromopyridinium]$_2$[Ru(bipy)(CN)$_4$]·2H$_2$O (**4**·2H$_2$O) showing the O−H···NC(Ru) hydrogen-bonded network and C−Br···O halogen bonds. Cations colored blue participate in halogen bonding, whereas cations shown in red do not but form a π-stacked arrangement with the bipy ligands of the anions. The C−Br···O halogen bonds are depicted as solid bonds colored with the atom colors (blue/purple); the O−H···N hydrogen bonds are shown by alternating black/white lines. (b) Enlarged view of part of the network showing (O−H···N and C−H···O) hydrogen bonds and C−Br···O halogen bonds associated with the two independent water molecules.

exclude water, yet complexes **2** and **3** crystallized with no lattice water molecules. This lack of lattice water molecules is previously unknown for salts of [Ru(bipy)(CN)$_4$]$^{2-}$ and its relatives which normally crystallize with numerous HOH···NC(Ru) hydrogen-bonding interactions present, even from non-aqueous solvents where very low levels of water are present;[7,8,11] the water-free species (PPN)$_2$[Ru(bipy)(CN)$_4$] is reported to be extremely hygroscopic[11] and has been used as a moisture sensor in both the solid state[11] and solution.[17] The implication is that in complexes **2** and **3** the charge-assisted C−I···NC(Ru) halogen-bonding interactions are sufficiently strong that they form in preference to HOH···NC(Ru) hydrogen bonds, although the obvious caveats about crystal structures being controlled as much by kinetic factors as by thermodynamic ones apply. In contrast, the structure of **4**·2H$_2$O exhibits no C−Br···NC(Ru) halogen bonds and in **5**·5H$_2$O there are only weak C−Br···π(NC) halogen bonds involving some of the C−Br groups, all of which participate in extensive C−Br···Br halogen bonding. These observations are consistent with the general pattern that C−Br groups are weaker halogen bond donors than C−I groups.[5a,b,18] Instead, HOH···NC(Ru) hydrogen bonds with lattice water molecules dominate the interactions of the anions in **4**·2H$_2$O and **5**·5H$_2$O as is typical for the [Ru(bipy)(CN)$_4$]$^{2-}$ anion.

Solution Studies. To see if the C−X···NC(Ru) interactions persisted in solution we performed UV/vis spectroscopic titrations in which portions of *N*-methyl-pyridinium-, *N*-methyl-3-bromopyridinium-, or *N*-methyl-3-iodopyridin-

(17) Pinheiro, C.; Lima, J. C.; Parola, A. J. *Sens. Actuators, B* **2006**, *114*, 978.

(18) (a) De Santis, A.; Forni, A.; Liantonio, R.; Metrangolo, P.; Pilati, T.; Resnati, G. *Chem.—Eur. J.* **2003**, *9*, 3974. (b) Walsh, P. L.; Ma, S.; Obst, U.; Rebek, J., Jr. *J. Am. Chem. Soc.* **1999**, *121*, 7973. (c) Messina, T.; Metrangolo, P.; Panzeri, W.; Ragg, E.; Resnati, G. *Tetrahedron Lett.* **1998**, *39*, 9069. (d) Metrangolo, P.; Panzeri, W.; Recupero, F.; Resnati, G. *J. Fluorine Chem.* **2002**, *114*, 27.

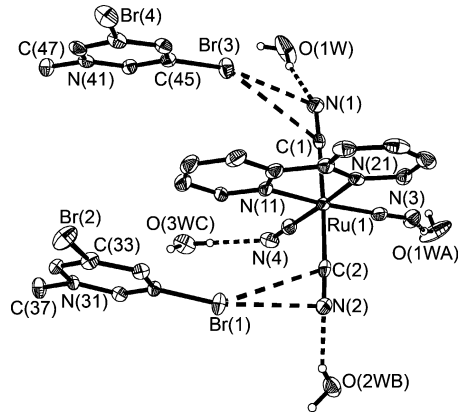

Figure 9. Atomic labeling scheme for the structure of [*N*-methyl-3,5-dibromopyridinium]$_2$ [Ru(bipy)(CN)$_4$]·5H$_2$O (**5**·5H$_2$O), with O−H···NC(Ru) hydrogen bonds and C−Br···π(CN) halogen bonds shown by dashed lines. The view emphasizes the coordination environment around the complex anion; the water molecule O(5W) is not shown for clarity and some of the H-bonded water molecules shown come from different asymmetric units from the complex anion. Thermal ellipsoids are at the 40% probability level.

ium hexafluorophosphate were added to a solution of [PPN]$_2$[Ru(4,4′-^{t}Bu$_2$-bipy)(CN)$_4$] in CH_2Cl_2. This complex, with two t-butyl substituents on the bipy ligand, is much more soluble in organic solvents than the parent unsubstituted complex used for the structural studies and therefore is ideal for UV/vis titrations to help avoid precipitation of the cation−anion combinations.[8e,19]

Interaction of the lone pairs of the cyanide groups with any Lewis acidic groups (protons in protic solvents[10] or polyammonium cations,[9a] or metal cations in non-competitive solvents[8e]) results in stabilization of the metal d(π) orbitals, and hence a blue shift of the Ru[d(π)]→bipy(π*) ^{1}MLCT absorption, and likewise a blue shift and increase in intensity of the consequent ^{3}MLCT emission. We expect that any C−X···NC(Ru) halogen bonding in solution will be signaled in the same way, since the interaction of the cyanide lone pairs with the electrophilic halogen atoms on the organic cations will be electron-withdrawing with respect to the complex anion.

Figure 11 shows the effect of addition of small portions of *N*-methyl-3-bromopyridinium hexafluorophosphate (up to 3 equiv) to a solution of [PPN]$_2$[Ru(4,4′-^{t}Bu$_2$-bipy)(CN)$_4$] in CH_2Cl_2 (8×10^{-5} M). A significant blue shift in the two ^{1}MLCT absorptions occurs, from 523 to 467 nm for the lower-energy absorption and from 364 to 343 nm for the higher-energy absorption. These equate to shifts of 2260 cm^{-1} and 1680 cm^{-1}, respectively. These shifts are modest compared to those that occur in the presence of water, or additional metal cations, which is to be expected; but they are approximately equivalent to what would be observed using ethanol as solvent.[10]

The inset to Figure 11 shows how the absorbance values at 470 and 330 nm, where the change in absorbance is at its largest, varies during the titration. These curves clearly do not follow the shape of a simple 1:1 binding isotherm but have a more complicated form, with sharp changes in slope

(19) Derossi, S.; Adams, H.; Ward, M. D. *Dalton Trans.* **2007**, 33.

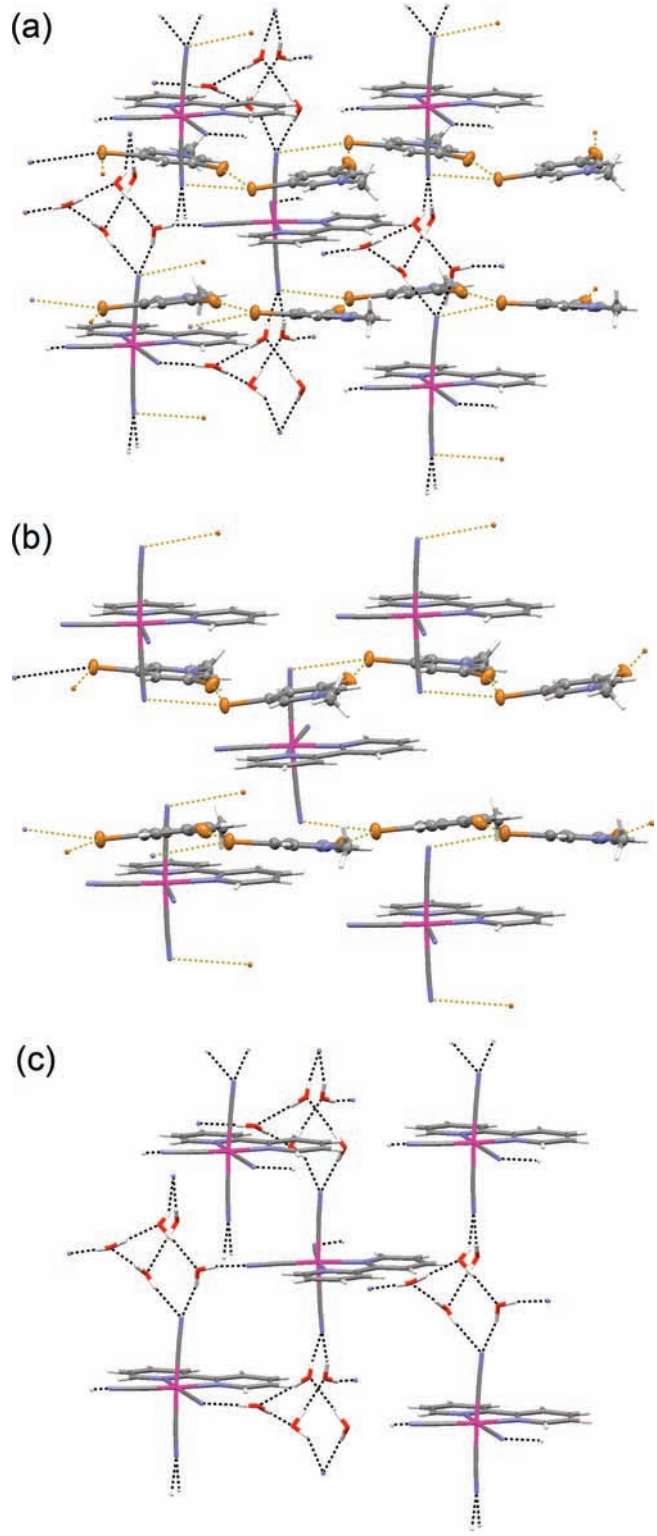

Figure 10. (a) Crystal structure of [*N*-methyl-3,5-dibromopyridinium]$_2$-[Ru(bipy)(CN)$_4$]·5H$_2$O (**5**·5H$_2$O) showing the hydrogen-bonded network (O−H···O and O−H···N) involving water molecules cyanide ligands and the halogen-bonded network (C−Br···Br and C−Br···N) involving C−Br groups of cations and cyanide ligands. (b) Hydrogen-bonded network shown with cations omitted. (c) Halogen-bonded network shown with water molecules omitted. A displacement ellipsoid representation (50% probability) is used for cation non-hydrogen atoms in Figures 10a and 10c. Hydrogen bonds are shown as black dashed lines. Halogen bonds are shown as brown dashed lines.

at about 1.0 and 1.5 equiv of cation. The shape of this curve indicates that there are multiple equilibria present involving

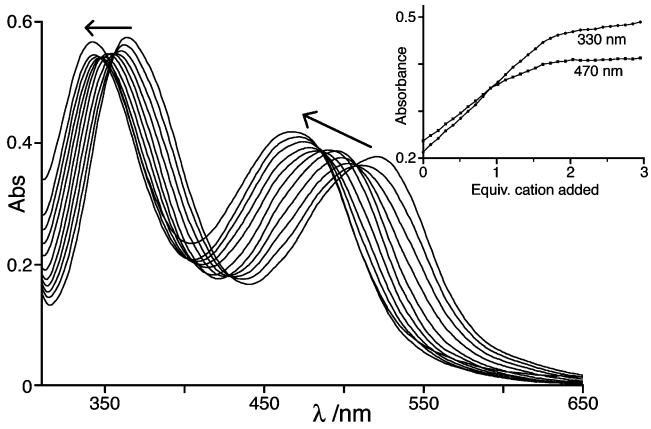

Figure 11. Changes in the UV/vis absorption spectrum of $[PPN]_2[Ru(4,4'\text{-}{}^tBu_2\text{-bipy})(CN)_4]$ in CH_2Cl_2 (8×10^{-5} M) on titration with *N*-methyl-3-bromopyridinium hexafluorophosphate. The inset figure shows the changes in absorbance at two wavelengths (330 and 470 nm) during the titration; on the latter of these the changes in gradient after addition of 1.0 equiv and then 1.5 equiv of *N*-methyl-3-bromopyridinium hexafluorophosphate are obvious.

Table 2. Calculated Cation/Anion Association Constants in CH_2Cl_2[a]

cation	K_{11}/M^{-1}	K_{23}/M^{-4}	K_{12}/M^{-2}
N-methyl-pyridinium	2×10^8	6×10^{26}	1×10^{13}
N-methyl-3-Br-pyridinium	8×10^7	8×10^{25}	4×10^{12}
N-methyl-3-I-pyridinium	2×10^7	6×10^{24}	3×10^{12}

[a] See main text for definitions of K_{11}, K_{23}, and K_{12}. Values are accurate to within an order of magnitude.

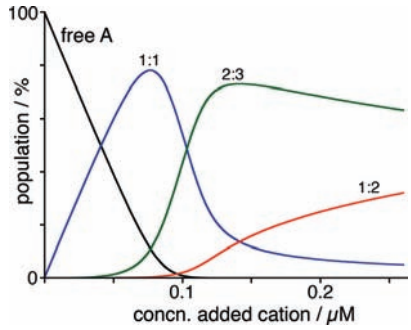

Figure 12. Speciation diagram for [*N*-methyl-3-bromopyridinium]$_2$-[Ru(bipy)(CN)$_4$], calculated from the UV/vis titration data in Figure 11.

at least four different states. The simplest interpretation that is consistent with the changes in slope at stoichiometric ratios of 1:1 and 1:1.5 (anion/cation) is that the four species are the free anionic metal complex $[Ru(4,4'\text{-}{}^tBu_2\text{-bipy})(CN)_4]^{2-}$, the 1:1 anion/cation adduct, a 2:3 complex with two anions and three bromopyridinium cations, and finally a much weaker 1:2 anion/cation adduct when the cation is present in large excess.

The formation of 1:1 and 1:2 complexes is simple enough to understand. It is to be expected that first one, and then a second, bromopyridinium cation will associate with the dianion, with the second association constant being much lower than the first for simple electrostatic reasons (the first association is between a cation and a dianion; the second is between a cation and a monoanion). It is interesting, however, that a well-defined 2:3 species forms at the intermediate stage; we can speculate that this has a cage structure in which each bromopyridinium cation bridges two cyanide ligands from a pair of complex anions, each of which

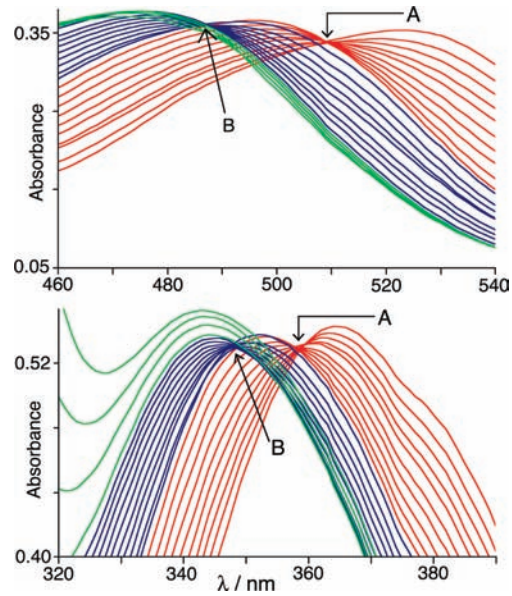

Figure 13. Details from the UV/vis titration of $[PPN]_2[Ru(4,4'\text{-}{}^tBu_2\text{-bipy})(CN)_4]$ with *N*-methyl-3-bromopyridinium in CH_2Cl_2 shown in Figure 11. The spectra corresponding to stepwise formation of the 1:1, 3:2, and then 2:2 cation/anion complexes are shown in red, blue and green respectively; **A** and **B** denote the isosbestic points during the first phase (red spectra) and second phase (blue spectra).

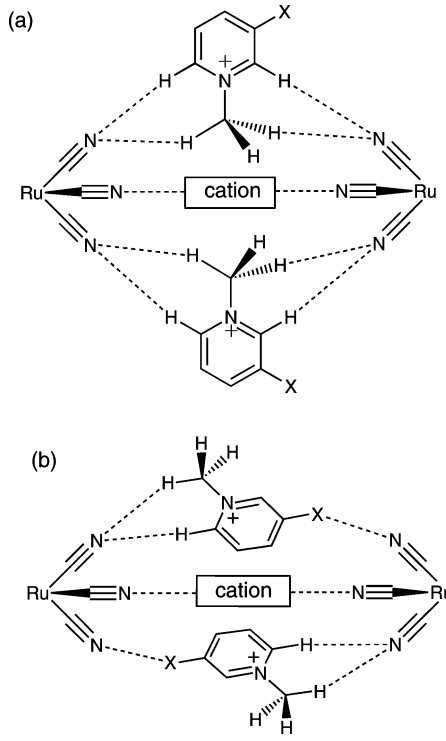

Figure 14. Two possible structures for the 3:2 cation/anion complex formed during the titration shown in Figure 11. In (a) each cation bridges both anions via hydrogen bonds; in (b) a combination of hydrogen bonding and halogen bonding (X = Br, I) is involved in the bridges (cf. Figure 6b).

use a *fac*-disposed set of three cyanides. Possible structures of this species are discussed further below. The values of the association constants obtained for the best fit of the experimental data to eqs 1−3 are reported in Table 2 (in eqs 1− 3, [A] is the concentration of free anion; [C] is the concentration of free cation; and [AC], [A_2C_3], and [AC_2] are the concentrations of the three adducts).

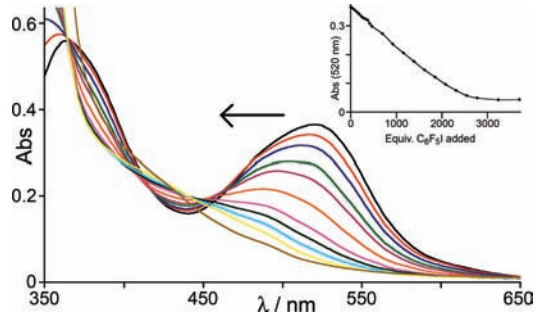

Figure 15. Evolution of the electronic spectra of [PPN]$_2$[Ru(4,4′-^{t}Bu$_2$-bipy)(CN)$_4$] in CH_2Cl_2 (8.1×10^{-5} M) on titration with a large excess of C_6F_5I; by the end of the titration the solvent volume was approximately 5% C_6F_5I.

$$K_{11} = \frac{[A][C]}{[AC]} \quad (1)$$

$$K_{23} = \frac{[A]^2[C]^3}{[A_2C_3]} \quad (2)$$

$$K_{12} = \frac{[A][C]^2}{[AC_2]} \quad (3)$$

The titration was carried out close to the tight binding limit to get reasonable intensities for the UV/vis absorptions, which limits the accuracy of the data analysis. However, the *relative* stabilities of the three complexes can be determined accurately from the data. The 1:1 [Ru(4,4′-^{t}Bu$_2$-bipy)(CN)$_4$]$^{2-}$/(*N*-methyl-3-bromopyridinium) complex is exceptionally stable, with a formation constant ($>10^7$ M^{-1}) stronger than observed in 1:1 adducts of [Ru(4,4′-^{t}Bu$_2$-bipy)(CN)$_4$]$^{2-}$ with alkali metal cations in MeCN.[8e] This initial 1:1 complex is replaced by the 2:3 cage complex as soon as sufficient cation becomes available, and then at higher cation concentrations, the 2:3 and 1:2 complexes are in equilibrium. The overall stability constants can be used to estimate the concentrations at which the three different complexes are formed: the 1:1 adduct forms at a complex concentration of about 10^{-7} M, the 2:3 complex forms at 10^{-6} M concentrations, and the 1:2 complex forms at concentrations of 10^{-5} M. The full speciation diagram is shown in Figure 12.

A closer look at the evolution of the UV/vis spectra of the [Ru(4,4′-^{t}Bu$_2$-bipy)(CN)$_4$]$^{2-}$ anion during the titration clearly shows the presence of these three distinct phases (Figure 13). Formation of the first 1:1 anion/cation adduct in the early stages (red spectra) is signaled by isosbestic points (labeled **A**) at 508 and 356 nm, followed by a shift in the lower-energy absorption maximum from 522 to 495 nm (ca. 1000 cm^{-1}) and the higher-energy one from 364 to 353 nm (ca. 900 cm^{-1}). The second phase (blue spectra) results in a loss of the first isosbestic point and formation of new ones at 487 and 348 nm (labeled **B**), as the 1:1 adduct is replaced by the 3:2 adduct; the absorption maxima shift to 476 and 345 nm. During the final phase (green spectra), the second isosbestic point is clearly lost, and the absorption maxima steadily shift slightly further to higher energy, to 467 and 343 nm, as the 1:2 adduct starts to dominate.[20,21]

The titration of [PPN]$_2$[Ru(4,4′-^{t}Bu$_2$-bipy)(CN)$_4$] with *N*-methyl-3-iodopyridinium hexafluorophosphate proceeds along exactly similar lines with the evolution of electronic spectra being almost superimposable. The two ^{1}MLCT absorptions (initially at 523 and 365 nm) are blue-shifted to 470 and 343 nm, shifts of about 2200 and 1800 cm^{-1} respectively (see Supporting Information). The shape of the plot of (ΔAbs) versus amount of cation added is the same and can be analyzed in exactly the same way, with formation of 1:1, then 3:2, and finally 2:1 anion/cation adducts, with the discrete steps apparent from changes in the isosbestic points in the UV/vis spectroscopic titrations. The stability constants for the complexes are very similar to those reported for the bromopyridinium complexes in Table 2, with the small differences being within the experimental error.

The similarity between the two sets of association constants using bromo- and iodo-pyridinium cations implies one of two things. Either specific interactions with halogen atoms are not significantly involved in the [Ru(4,4′-^{t}Bu$_2$-bipy)(CN)$_4$]$^{2-}$/halopyridinium association, which is dominated by other factors such as ion pairing; or, both C−I···NC and C−Br···NC halogen bonding are occurring but have about the same strengths. The latter explanation is the less appealing: the crystallographic evidence from our study and that of others suggests that C−I···NC interactions should be the stronger, and other halogen bonding interactions have been clearly demonstrated to be stronger when iodine atoms are involved compared to those involving bromine atoms.[5a,b,18] We are left with the conclusion that the strong association between [Ru(4,4′-^{t}Bu$_2$-bipy)(CN)$_4$]$^{2-}$ anions and halopyridinium cations in CH_2Cl_2 solution is independent of the nature of the halogen atom because it is dominated by electrostatic ion-pairing effects. Actually we cannot be sure that the halogen atoms are even involved in cation/anion contacts in solution: it is also possible that C−H···NC(Ru) hydrogen bonds to the aromatic cation occur (see below), which will be more or less independent of the nature of the halogen substituent elsewhere on the cation.

To clarify this issue we performed two control experiments. First, we used the non-halogenated *N*-methyl-pyridinium cation in a similar UV/vis titration and found that it behaved almost identically to the halogenated cations. The shift of UV/vis spectra to higher energy, including the clear set of steps associated with formation of 1:1, 3:2, and then 2:1 cation/anion species, is very similar to the sequence of spectra observed with either of the halogenated cations (see Supporting Information), and the calculated magnitudes of the association constants are also comparable (Table 2).

(20) We note that there is no evidence for an additional [Ru(4,4′-^{t}Bu$_2$-bipy)(CN)$_4$]$^{2-}$ → pyridinium charge-transfer band, which might be expected, cf. the titration of hexacyanoferrate(II) with a pyridinium cation which generated a hexacyanoferrate(II) → pyridinium charge-transfer transition at the blue end of the visible region of the spectrum (ref 21). However, this CT transition was weak ($\varepsilon = 41$ M^{-1} cm^{-1}), and such a transition would be obscured by the MLCT transitions associated with the [Ru(4,4′-^{t}Bu$_2$-bipy)(CN)$_4$]$^{2-}$ complex which are two orders of magnitude more intense.

(21) Kunkely, H.; Vogler, A. *Inorg. Chim. Acta* **2000**, *300−302*, 1090.

Clearly, therefore, the main contribution to the high cation/anion association constants in solution is the electrostatically driven ion-pairing, with the specific nature of the interaction at the point of contact (halogen bond or hydrogen bond) making a minor contribution to the binding constants. This is in agreement with the lower association constants for halogen bonds determined from solution measurements when neutral species are involved.[3f,4e]

A recent theoretical study showed that association of anions with *N*-methyl-pyridinium cations occurred principally at two positions: close to H^3/H^5, and in the region between H^2/H^6 and the methyl protons.[22] Our own calculation of the charge distribution for an *N*-methyl-pyridinium cation in CH_2Cl_2 solution is consistent with this, showing the methyl protons to have the highest $\delta+$ charge (0.21 units each) with the aromatic ring protons being marginally less $\delta+$ (0.15−0.19 units each, with the H^3/H^5 protons having marginally the highest $\delta+$ charge), see the Supporting Information.

On this basis, possible structures for the 3:2 cation/anion intermediate are shown in Figure 14, in which each methyl-pyridinium cation bridges two cyanoruthenate anions. A *fac* array of three cyanide ligands from each of the two anions could be involved to give a cage-like structure. It is not geometrically possible for four such bridging interactions to occur simultaneously because the axial pair of cyanide ligands on the anion are mutually *trans*, but a set of three facially related cyanide ligands could be involved, resulting in the observed 3:2 cation/anion stoichiometry. The association of the cyanide groups from the anion with the cation could involve hydrogen bonding and/or halogen bonding, as sketched; we note that the arrangement involving one hydrogen-bonding and one halogen-bonding interaction for each bridging cation is exactly similar to what occurs in the solid state for one of the cations in Figure 6b which bridges two complex anions in this manner.

As the second control experiment we used pentafluoroiodobenzene as the halogen-bond forming agent: being neutral (and fluorinated) there will be no ion-pairing or hydrogen-bonding effects, but this molecule is optimized for forming CN···I halogen bonds involving a neutral molecule. In this case huge excesses of C_6F_5I were required to cause small changes in the UV/vis spectrum of $[Ru(4,4'\text{-}^tBu_2\text{-bipy})(CN)_4]^{2-}$ during the titration, with the MLCT band slowly flattening out and becoming less distinct as the titration proceeded (Figure 15)—a quite different spectroscopic response from that shown using the pyridinium cations. Over 3000 equiv of C_6F_5I were required until there was no further change observed. The data do not fit well to a simple 1:1 or a non-cooperative 4:1 binding isotherm, but if we assume a simple pairwise interaction, we can estimate an association constant of approximately 6 M^{-1}. The process is probably best described by a weak association, followed by cooperative solvation of the anion at higher concentrations of the guest (0.2 M). This would account for the abrupt change in behavior at this point in the titration, but the very nature of the solvent has changed by the time these concentrations are reached. The C−I···NC(Ru) halogen bonding interaction with C_6F_5I in CH_2Cl_2 solution is, therefore, negligible in strength compared to the charge-assisted interactions involving the *N*-methylpyridinium cations (with or without halogen substituents).

Finally, we examined the changes in luminescence spectra of $[Ru(4,4'\text{-}^tBu_2\text{-bipy})(CN)_4]^{2-}$ during the titration with the *N*-methylpyridinium cations. In non-protic solvents the complex anion has very weak luminescence (at 760 nm in CH_2Cl_2).[10] Addition of hydrogen-bond donors or metal cations, which interact with the externally directed cyanide lone pairs, moves this ^{3}MLCT luminescence to higher energy as the d(π) orbitals are stabilized, with a concomitant substantial increase in intensity and lifetimes of the luminescence.[8e,9a,10] During the titration with the *N*-methyl-pyridinium cations, however, we see different behavior. The ^{3}MLCT emission band does move to higher energy by about 2000 cm^{-1} (to 660 nm) as a consequence of the ion-pairing, in line with the blue-shifts observed in the absorption spectra. However, the luminescence does not grow in intensity but remains very weak, ending up at about the same intensity as it started. We ascribe this to partial quenching of the ^{3}MLCT excited-state by photoinduced electron-transfer to the *N*-methyl-pyridinium cations in the ion-paired assemblies. The low Ru(II)/Ru(III) redox potential of $[Ru(bipy)(CN)_4]^{2-}$ and its relatives in non-protic solvents[7,10] means that oxidation to Ru(III) is facile, such that the excited state is a particularly good electron donor (better than $[Ru(bipy)_3]^{2+}$),[7] and photoinduced electron-transfer to an adjacent pyridinium cation will therefore be thermodynamically favorable.

Conclusions

In the solid state, C−I···NC(Ru) halogen bonds dominate the structures of complexes **2** and **3**, which are based on combination of the $[Ru(bipy)(CN)_4]^{2-}$ anion with *N*-methyl-3-iodopyridinium and *N*-methyl-3,5-diiodopyridinium cations respectively. However, replacement of I atoms with Br atoms, using the cations *N*-methyl-3-bromopyridinium and *N*-methyl-3,5-dibromopyridinium in **4** and **5**, respectively, results in no comparable C−Br···NC(Ru) interactions in the solid state. In CH_2Cl_2 solution strong association between $[Ru(4,4'\text{-}^tBu_2\text{-bipy})(CN)_4]^{2-}$ and various *N*-methyl-pyridinium cations, with or without halogen substituents, occurs, with the association being dominated by electrostatic ion-pairing effects, such that the presence or absence of a halogen makes no significant difference to the association stoichiometry or strength. The cation−anion association occurs in clear stages, with 1:1, 3:2, and 2:1 cation/anion adducts forming at different concentrations. This association results in a blue shift of the ^{1}MLCT absorption maxima of the $[Ru(4,4'\text{-}^tBu_2\text{-bipy})(CN)_4]^{2-}$. This destabilization of the ^{1}MLCT state is accompanied by a blue-shift in the resulting ^{3}MLCT luminescence, but the luminescence intensity is very weak, probably because of photoinduced electron-transfer to the pyridinium groups in the cation−anion assemblies. We conclude that charge-assisted C−X···NC(Ru) halogen bonds are useful synthons for control of the solid state structures of crystalline cyanometallate-halopyridinium assemblies

(22) Zhu, X.-Y.; Zhang, D.-J.; Liu, C.-B. *Acta Chim. Sinica* **2007**, *65*, 2701.

when X = I, and even compete with hydrogen-bonded solvate formation, whereas when X = Br solvate formation can dominate. The halogen atoms do not, however, control cation−anion assembly in CH_2Cl_2 solution, where ion-pairing dominates and the presence or absence of a halogen atom on the cation makes little difference to the solution speciation behavior.

Experimental Section

Syntheses. Pyridinium Salts. [*N*-methyl-3-iodopyridinium](PF_6) and [*N*-methyl-3-bromopyridinium](PF_6) were prepared from aqueous solutions of the known iodide salts[23] by addition of aqueous NH_4PF_6 (2 equiv) followed by concentration of the solution. On standing the products precipitated as colorless crystals. [*N*-methyl-3,5-dibromopyridinium](PF_6) was similarly prepared by addition of two equiv of aqueous NH_4PF_6 to an aqueous solution of the known tetrafluoroborate salt.[24] [*N*-methyl-3,5-diiodopyridinium](PF_6) was prepared in two steps, by initial alkylation of 3,5-diiodopyridine[25] with (Me_3O)(BF_4) to give [*N*-methyl-3,5-diiodopyridinium](BF_4),[24] followed by anion metathesis with aqueous NH_4PF_6 as above to give a colorless crystalline solid. In all cases satisfactory analytical and spectroscopic data were obtained for these simple salts.

Compounds 1−5. These were all prepared in the same way by mixing together a solution of $(PPN)_2$[Ru(bipy)$(CN)_4$][11] in CH_2Cl_2 with a solution containing two equiv of the appropriate *N*-methylpyridinium salt in the same volume of MeCN. Slow evaporation resulted in every case in an amorphous red precipitate in which a small number of crystals of the desired product were embedded and could be extracted manually; the identity of these was confirmed by ES mass spectrometry which showed in each case the expected peak for the [Ru(bipy)$(CN)_4$]$^{2-}$ anion in negative-ion mode and for the appropriate *N*-methylpyridinium cation in positive ion mode.

Spectroscopic Studies. UV/vis and luminescence spectroscopic titrations were carried out using 8×10^{-5} M solutions of $[PPN]_2$-[Ru(4,4′-^{t}Bu$_2$-bipy)$(CN)_4$][19] in CH_2Cl_2, to which was added in small portions a 10^{-3} M solution of the appropriate *N*-methylpyridinium salt. This solution also contained 8×10^{-5} M $[PPN]_2$[Ru(4,4′-^{t}Bu$_2$-bipy)$(CN)_4$] such that there was no dilution of the $[PPN]_2$[Ru(4,4′-^{t}Bu$_2$-bipy)$(CN)_4$] as the *N*-methylpyridinium salt is titrated in. UV/vis spectra during the titrations were recorded with Cary 50 spectrophotometer; luminescence spectra were recorded using a Jobin-Yvon Fluoromax 4 fluorimeter, using in each case an excitation wavelength at which the absorption was 0.1 units, to compensate for the changes in the UV/vis spectra during the titration.

Curve fitting of the UV/vis titration data to calculate stepwise association constants, according to the scheme outlined in the main text, was performed using purpose-written software on an Apple Macintosh computer. The values of the association constants of all of the species present, and the resulting speciation diagrams, were obtained by fitting the experimental titration data to the calculated UV/vis absorption intensity using a Simplex optimization procedure to minimize the sum of the squares of the differences between the calculated and experimental values.[26]

X-ray Crystallography. Suitable crystals of **1−5** were mounted in a stream of cold N_2 on a Bruker APEX-2 CCD diffractometer equipped with graphite-monochromated Mo Kα radiation from a sealed-tube source. Details of the crystal, data collection and refinement parameters are summarized in Table 1, and selected structural parameters are provided in the Supporting Information. Data were corrected for absorption using empirical methods (SADABS) based upon symmetry-equivalent reflections combined with measurements at different azimuthal angles.[27] The structures were solved by direct methods and refined by full-matrix least-squares on weighted F^2 values for all reflections using the SHELX suite of programs.[28] Non-hydrogen atoms were refined anisotropically. Hydrogen atoms were placed in calculated positions, refined using idealized geometries (riding model), and assigned fixed isotropic displacement parameters.

Calculations. The charge distribution for the *N*-methylpyridinium cation in CH_2Cl_2 was calculated using GAUSSIAN;[29] for full details see the Supporting Information.

Acknowledgment. We thank the EPSRC (UK) and the University of Sheffield for financial support, and Dr. Anthony Meijer (Sheffield) for the calculation of the charge distribution in the *N*-methylpyridinium cation.

Supporting Information Available: Further details are given in Tables S1−S5 and Figures S1 and S2. Crystallographic data is given in CIF file format. This material is available free of charge via the Internet at http://pubs.acs.org.

IC8021529

(23) Barlin, G. B.; Benbow, J. A. *J. Chem. Soc., Perkin Trans. 2* **1974**, *7*, 790.
(24) Logothetis, T. A.; Meyer, F.; Metrangolo, P.; Pilati, T.; Resnati, G. *New J. Chem.* **2004**, *28*, 760.
(25) Winkler, M.; Cakir, B.; Sander, W. *J. Am. Chem. Soc.* **2004**, *126*, 6135.
(26) Nelder, J. A.; Mead, R. *Comp. J.* **1965**, *7*, 308.
(27) (a) Sheldrick, G. M. *SADABS, Empirical absorption correction program*; University of Göttingen: Göttingen, Germany, 1995; based upon the method of Blessing.[27b](b) Blessing, R. H. *Acta Crystallogr.* **1995**, *A51*, 33.
(28) Sheldrick, G. M. *Acta Crystallogr.* **2008**, *A64*, 112.
(29) Frisch, M. J. et al. *Gaussian 03*, Revision C.02; Gaussian, Inc.: Wallingford, CT, 2004.